XL CILAMCE
IBERO-LATIN AMERICAN CONGRESS ON COMPUTATIONAL METHODS IN ENGINEERING
NOVEMBER 11-14, 2019
Praiamar Natal Hotel & Convention Natal, RN-BRAZIL

# ANALYSIS OF SLOSHING SUPPRESSORS IN LIQUEFIED NATURAL GAS CARRIERS TANKS

**Danilo de A. Barbosa**
**Fabio P. Piccoli**
*danilofisico@yahoo.com.br*
*fabio_p_p@hotmail.com*
*Instituto Federal de Educação, Ciência e Tecnologia da Bahia*
*Instituto Federal de Educação, Ciência e Tecnologia do Espírito Santo*
*Rodovia Ilhéus-Itabuna, km 13, S/N -BRASIL, Ilhéus - BA, 45603-255*
*Av. Rio Branco, 50 - Santa Lucia, Vitória - ES, 29056-25*
**Daniel dos Santos Moreira**
**Thiago N. Barbosa**

**Abstract.** The problem of sloshing has been studied in the last decades, seeking to reduce the deleterious effects promoted by this phenomenon in liquefied natural gas carriers tanks. Since there is a need to develop tank designs capable of reducing the damaging effects of sloshing, a study on the hydrodynamic loads involving the fluid-structure relationship becomes necessary. In this work, attenuation devices were installed to reduce the effect of sloshing on containers, such as deflector blades positioned on tank walls. Regarding this topic, our work was devoted to testing two types of sloshing suppressor bulkheads, where two different heights were assigned and tested for the first vertical deflector located in the center of the tank. Secondly we change the morphology of the baffle, leaving it in the shape of an arrow pointing upwards. The results show that the baffles can be efficient mechanisms for the suppression of slonging and that there is a strongly relationship between the height of the baffles and the level of fluid filling in relation to the tank.

Keywords: Baffles, Arrow Baffles, Sloshing, Smoothed Particle Hydrodynamics.

# 1 Introduction

There is a question that has long been studied regarding sloshing and suppression of its effects: To what extent are the baffles capable of suppressing the hydrodynamic loads produced by the tank oscillations?

Although there have been reports of sloshing since the nineteenth century [1,2,3,4], this theme gained more prominence during the aerospace running [5,6]. And its effects have been studied with enough intensity in the last decades, in which it seeks to reduce the harmful effects promoted by this phenomenon in vessels, aircraft, and artificial satellites and also benefit buildings in earthquake-prone regions. Abramson (1969) studied the sloshing and suppression mechanisms, which presented fateful examples where spacecraft and satellites had problems during flight due to sloshing. The author also examined the various types of sloshing deflector mechanisms in storage tanks for propellant fuels from satellites or aircraft. Thus, it was sought to find the hydrodynamic loads acting on the vehicle structure or on the suppression devices after the fluid displacement. For this, the cylindrical and spherical and conical geometries with and without baffles were tested by the author. At the time, the effects produced by sloshing had already been known in which some that effects is the resonance induced fatigue and vehicular instability (vessel/watercraft), caused by hydrodynamic loading and oscillation of the fluid portion mass center.

There are also reports of accidents caused by sloshing in marine vessels [7], whose sloshing problem is involved in ships and fishing boats accidents, like the that occurred with the GAUL fishing boat in February 1974 and the happened with the Artic Rose fishing boat, which sank on April 2, 2001, giving rise to environment damage with fuel spillage.

The investigations after respective shipwrecks revealed that the vessels sank rapidly due to the dynamical effect of the free surface of the water associated with the flooding inside the compartments as the liquid starts to move freely [7]. Therefore, studying sloshing requires estimating how the pressure is distributed and how to control the external forces involved. This pressure in confined liquids caused by the transfer of movement amount from the container to the fluid is proportional to the container change rate velocity and to the free surface movement [8,9]

Another approach applies to the increasing exploration and exploitation of offshore oil and consequent increase in the number of Floating Production Storage and Offloading, FPSO platforms, and vessels to transport this fluid. Under standard conditions of fluid mass transport, the sloshing can produce a negative effect on the structures due to the dynamic loads that are generated, from which they can generate serious damages to boats.

Tsukamoto[10] states that to reduce the sloshing effect in containers attenuation devices such as deflector blades positioned on the walls and the roof or bottom of the tanks should be installed. Although, according to the author, these mechanisms were only effective at low fill levels. Considering the description above there is a need to develop tank designs capable of reducing the sloshing damaging effects. In addressing this topic, our work was concerned with testing two types of sloshing suppressor bulkheads, in which for the first vertical baffle, located at the center of the tank, it was assigned and tested two different heights. Afterward, we changed the morphology of the baffle, leaving it in the form of an arrow pointing upwards.

In order to assist us in the tests, we used the smoothed particle hydrodynamics SPH methods [10,11,12,13] and simulated the experimental work of Kishev et. al.[14].

# 2 Experimental Setup – Kishev et al.[14]

The rectangular tank used in the experiments made of Plexiglas was 60cm wide, 30cm high and 10cm deep. The tank has no internal structure so that it simulates a smooth tank of the type existing in

membrane-type LNG carriers. On each sidewall of the tank, several positions were prepared for pressure gauges. There were ten possible positions on each tank wall. Two pressure gauges with different sensitivities were used. The sidewalls of the tank were fitted with metal (copper) plates to prevent thermal shock on the gauges when passing from air to water. Such a metal plate was also added to the tank roof for the last group of experiments to measure pressures on the roof without thermal shock on the gauges. In that case, a small tank filled with water was also added on top. A high-speed video camera was mounted on a frame moving with the tank (Figure 1).

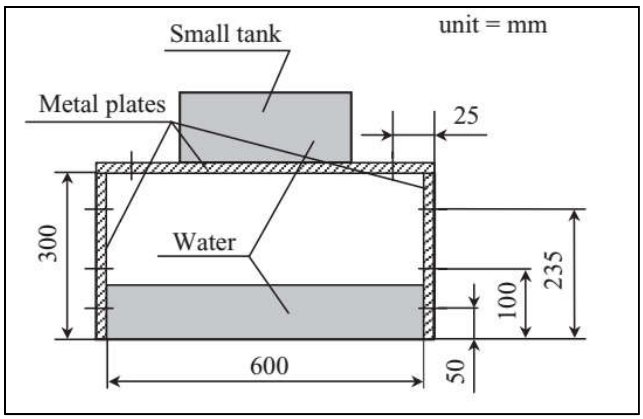


Figure 1: Experimental Setup. Font: Kishev et al. [14].

## 3 Numerical Setup

Kishev et al. [14] performed numerical experiments based on the Eulerian Constraint Interpolation Profile (CIP) and its variants and compared it against their physical experiments. That experiment consisted of a 60 x 30 x 10 cm tank. Now we reproduce the kinematic and dynamic appreciation with the SPH-COULOMB, taking advantage to test different values of beta and alpha of the artificial viscosity. In addition to using the experimental results obtained by Kishev et al.[14]to validate our model, we also compared the results with those found by Gotoh et al. [15] for the same configuration.

$$A = A_{max}\sin(2\pi\frac{t}{T})$$

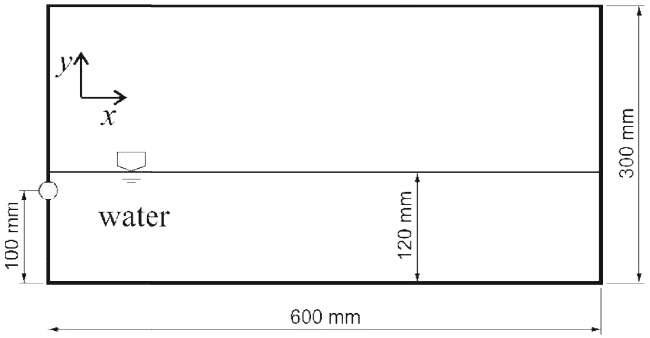


Figure. 2. Geometric description of the Kishev et al [14].

During the experiment, the tank was partially filled with water, around 12 cm (or 120 mm) deep. The maximum range of motion was 5 cm, while the excitation period was 1.3 s. Our simulation consists of several scenarios. Tanks were tested with virtual particles to simulate the contour. The domain particles has 0.006 m diameter. Fig. 3 shows this configuration after the first time step.

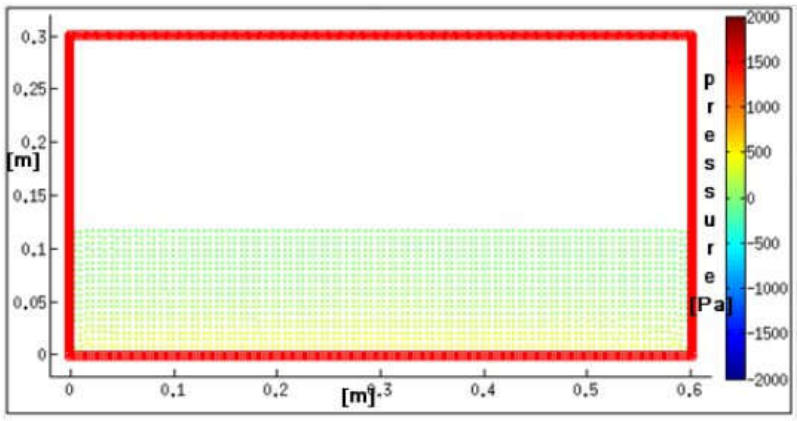


Fig. 3 Configuration at the instant 0.05 seconds with the null beta factor. Maximum pressure of 480.18 N / m² (Pa).

## 4 Mathematical Modelling.

The mathematical formulation applied to sloshing problem is, as part of the natural's phenomena, based on the fundamentals of the conservation laws of classic mechanics. Fortunately, the laws governing hydrodynamic phenomena can be expressed concerning mathematical equations, which, in general, are partial differential equations. In this case, the equations governing the phenomenon are the conservation of mass (Eq. 1) and conservation of momentum (Eq. 2).

Conservation of mass Equations:

$$\frac{D\rho}{Dt} = -\rho \frac{\partial u_i}{\partial x_i} \tag{1}$$

where $\rho$ is the density, $u_i$ is the velocity, $t$ is the time , and $x_i$ is the coordinate in the Cartesian plane or in three-dimensional $i = 1, 2, 3$ .

Conservation of Momentum

$$\frac{Du_i}{Dt} = -\frac{1}{\rho}\frac{\partial P}{\partial x_i} + \frac{1}{\rho}\frac{\partial \tau_{ij}}{\partial x_j} + g_i \tag{2}$$

where

$$\tau_{ij} = 2\mu\left(\frac{\partial u_i}{\partial x_j} + \frac{\partial u_j}{\partial x_i}\right) \tag{3}$$

where $P$ is the pressure, $\mu$ is the kinematic viscosity, and $g_i$ is the external force. The second term of the Eq. 2 is the surface force due to pressure per unit mass, and the third term is the force due to surface shear stress (or due to viscosity) per unit mass.

,

### 4.1 State Equation of Artificial Compressibility

In the SPH method, an artificial compressibility technique is used to model the incompressible flow as a slightly compressible flow. According to Liu & Liu [13], there are two ways to impose the incompressibility: by Eq. (4), which is used for cases involving low Reynolds Numbers incompressible flows using SPH; and by Eq. (5), Tait equation, which is applied to model free surface flows.

$$P = c^2 \rho \tag{4}$$

$$P = \beta \left[ \left( \frac{\rho}{\rho_0} \right)^{\gamma} - 1 \right] \tag{5}$$

Where $\beta = c^2 \rho_0 / \gamma$ and $\gamma$ is a constant (equal 7 in most circumstances), $\rho_0$ is the reference density, and $c$ is speed of sound in water. $\beta$ is a problem dependent parameter, which sets a limit for the maximum change of the density. In most circumstances, $\beta$ can be taken as the initial pressure [12].

## 5 BOUNDARY TREATMENT

Most Smoothed Particle Hydrodynamics (SPH) models usually treat the domain boundary with the use of virtual particles (or ghost particles). These particles are "placed" on the domain limits. Thus, a repulsive force is attributed to them to avoid interpenetration. Classically, the repulsive force used is derived from the Lennard-Jones' (LJ) potential, widely employed in molecular dynamics [11,12,13,16].

An alternative to the LJ force presented in this paper is the Coulomb force ( $F^{Coulomb}$ ) [16,17], Eq. 6, which, like the classical LJ technique, has the sole and exclusive purpose of keeping the particles inside the domain delimited by the virtual particles. Similar to the previous case, the polarization (or neutralization) has the same nature of the virtual particles, i.e., virtual and numerical, and therefore it does not allow physical discussion.

$$F_i^{Coulomb} = \begin{cases} k \dfrac{\left|Q^a\right|\left|Q^b\right|}{\left(x^2 + y^2 + z^2\right)^{3/2}} \left( x^2 e_i + y^2 e_j + z^2 e_k \right) & , r^{ab} \le r_o \\ 0 & , r^{ab} > r_o \end{cases} \tag{6}$$

were $\hat{r}_i = \dfrac{r_i}{|r_i|}$ and $|r_i| = r$ and $r^{ab} = \left\| x_a^i - x_b^i \right\|$ and $r_o$ é o cutoff

## 6 Results

Four types of tests were performed: (1) - tank without baffle; (2) - tank with the 0.05 meters defector; (3) - tank with a strap of 0.1 meters and (4) - tank with a screen in the shape of an arrow. Fig. 4 compares the first three scenarios. The negative scale was purposely used to verify the non-physical fluctuations of pressure.

In both Figs. 4 and 5, and yet table 1 is possible to notice that 0.05 meters barrier proved to be inefficient. The 0.1 meters bulkhead showed a greater attenuation of the hydrodynamic load on the walls. Another configuration was tested with a change in the morphology of the arrow-shaped bulkhead (Fig. 6).

For the same instant of time, the arrow-shaped baffle (Fig. 6) proved to be more efficient for sloshing suppression when compared to all other scenarios. In the region of the bulkhead, the hydrodynamic load is greater, reducing the effect of the pressure on the tank walls.

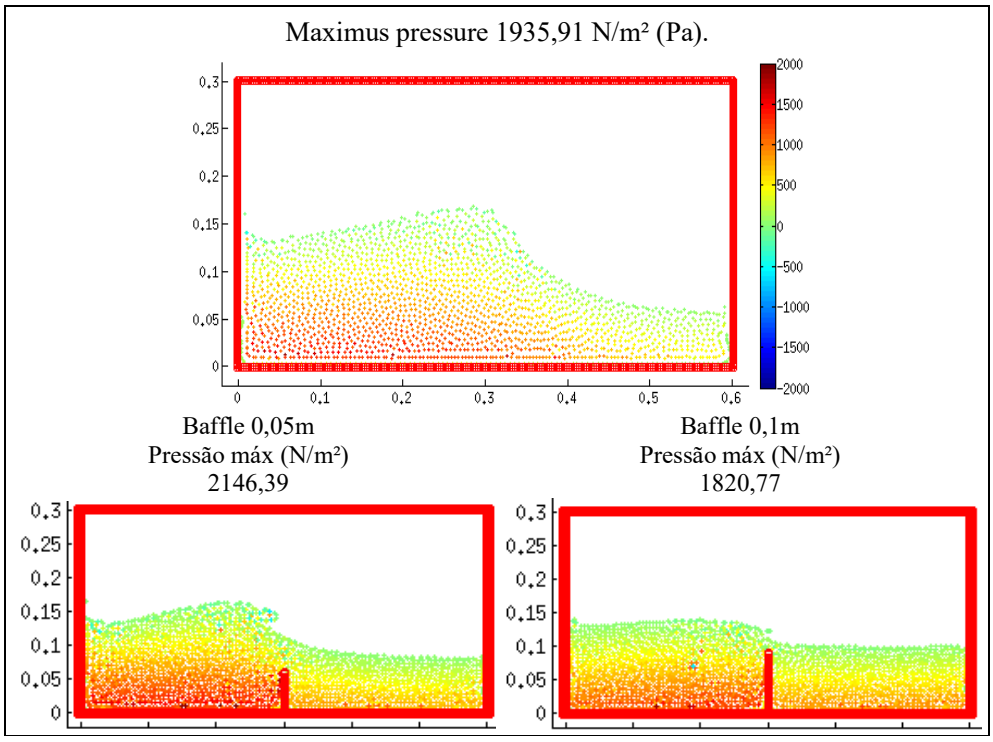


Fig. 4. At the top setting without the screen. In (b) bulkhead with 0.05 meters and the same configuration with bulkhead of 0.1 meter are showed in (c).

Table 1 – Pressure dates to figures set up 4 and 5

| Setup | Figure 4 | Figure 5 |
|---|---|---|
| Baffle's height (m) | Max Pressure (Pa) | Max Pressure (Pa) |
| without baffle | 1935,91 | 5569,18 |
| 0,05 | 2146,39 | 3096.41 |
| 0,1 | 1820,77 | 1942,76 |

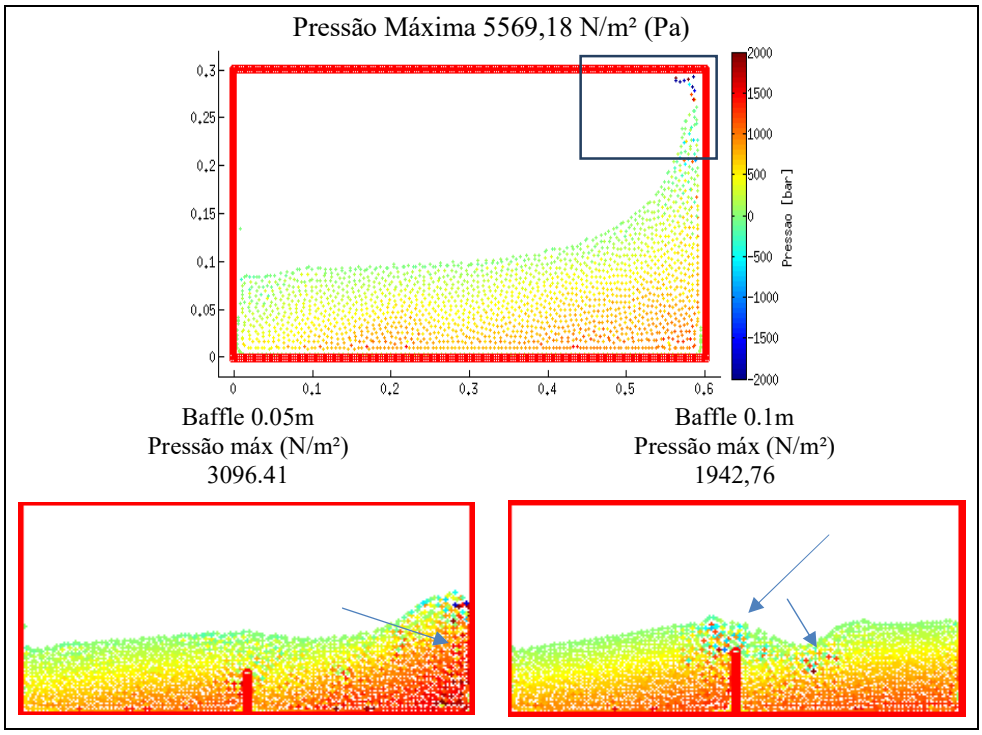


Fig. 5. The same configuration of figures 4, therefore when occurs the run up. In highlighter , small non-physical fluctuations of pressure.

Another configuration was tested with change in baffles morphology to "arrow" shape (Figure 6). At the same time, the baffle arrow was more efficient for sloshing suppression when compared to all other scenarios (Table 2). In the bulkhead region, the hydrodynamic load is higher, reducing the effect of pressure on the tank walls.

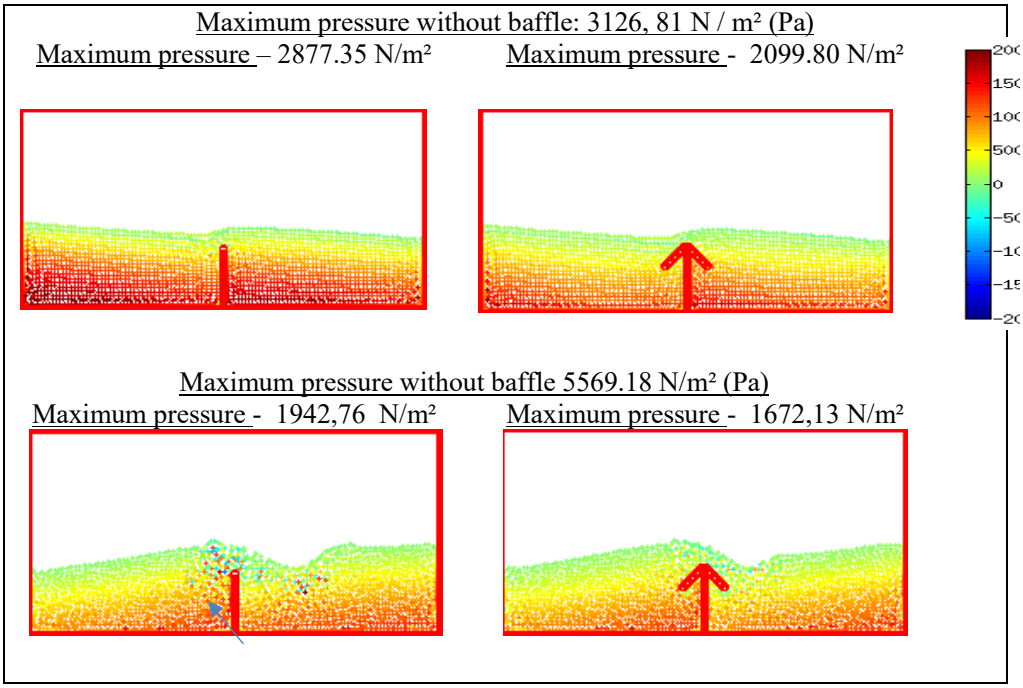


Fig. 6 - Comparison of the flow pressure field with baffles in different morphologies.

Table 2 - Comparison between vertical baffle and arrow-shaped arrow.

| *Baffle*s Shape | Max pressure (Pa) |
|---|---|
| whitout baffles | 5569,18 |
| Vertical 0,1m | 1942,76 |
| Arrow 0,1m | 1672,73 |

### 6.1 Pressure Quantification

Before quantifying the pressure, a qualitative comparison with the results obtained by Gotoh et al., [15] was performed. To simulate the physical configuration, those authors considered particles with a diameter of 3 mm - about 8000 particles. While in this work the diameter was 6 mm, corresponding to 2000 domain particles. They tested two different techniques and a slight underestimation of pressure is highlighted in Figure 7.

The Figure 8 compares the numerical experiments with the physical experiment by Kishev et. al [14]. For more information on method modifications see Gotoh et al. [15]

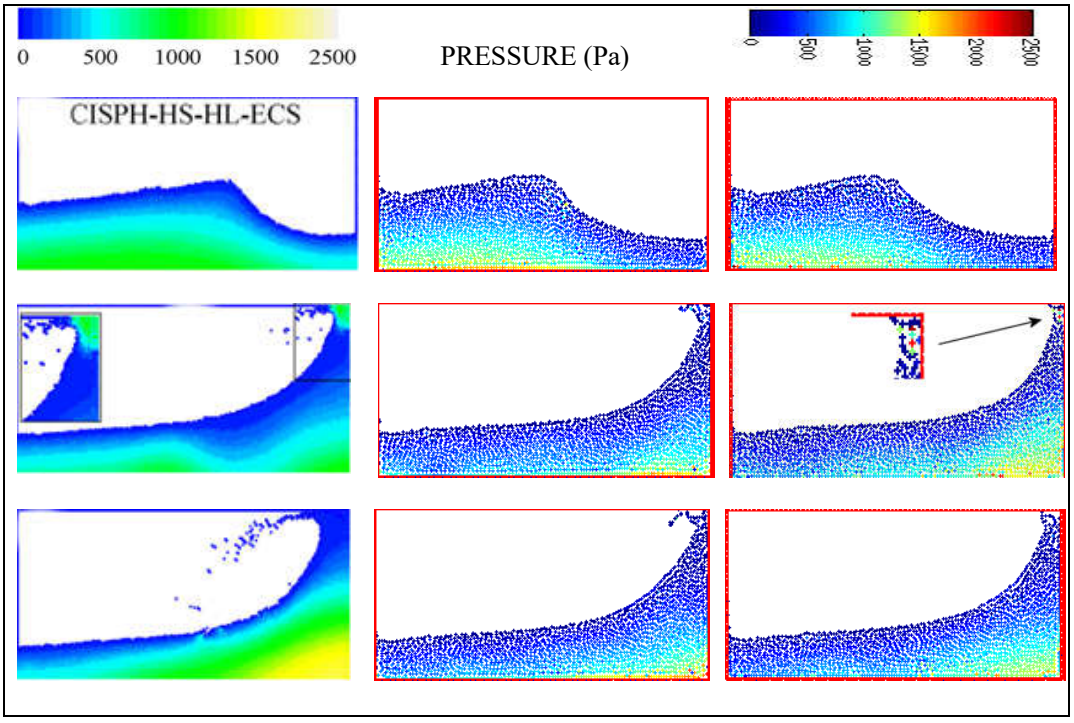


Figure 7. In the center, the flow with 1405 boundary particles and to the right of the center 705 virtual particles. Center left, modified SPH (ISPH) tested by Gotoh et. al, [15]. Rectangular Highlight refers to a small "underestimation" of pressure, which was also found by us.

Despite the morphological aspect of the configuration where the 1405 virtual particle boundary treatment is closer to the actual flow profile, the use of 705 ghost particles showed better approximations under the estimate for the flow dynamics values. Figures 9 and 10, for example, draw a quantitative parallel between the pressures encountered during the experiment by Kishev et al. [14] with the numerical technique used by him and with the one used and modified in this work.

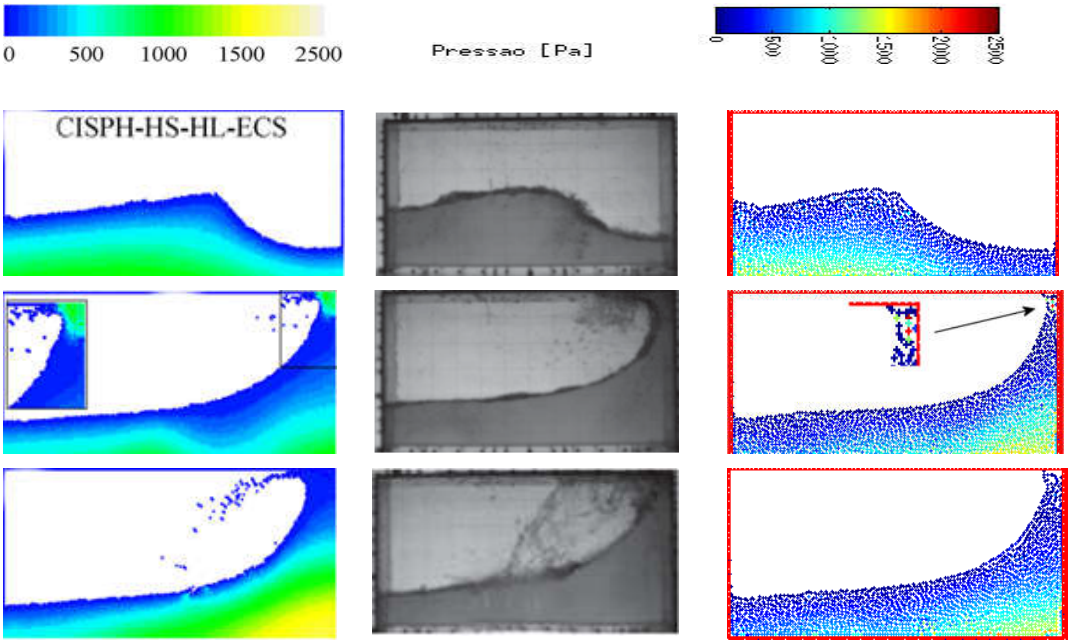


Fig. 8. The left center plots, flow profile described by Gotoh et al.[15]. At the center plots the experiment of Kishev et al.[14]. To the right, our contribution. The quantitative relation is performed in Fig. 9.

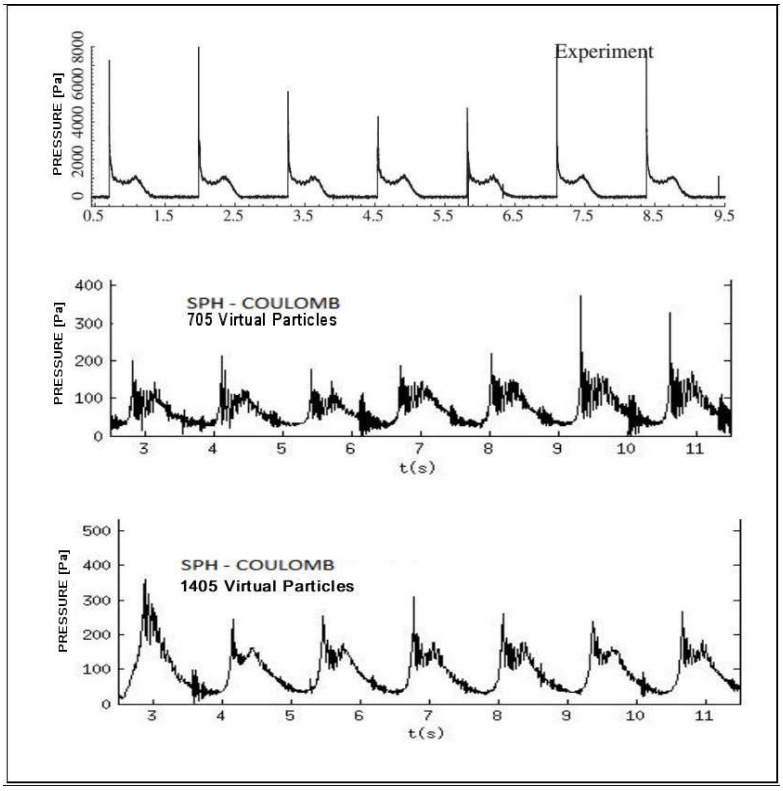


Figure 9 - At the top, it corresponds to the values collected from the physical experiment by Kishev et al. [14] Below in the center, SPH with 705 virtual particles. The third figure (top to bottom), SPH with 1405 virtual particles.

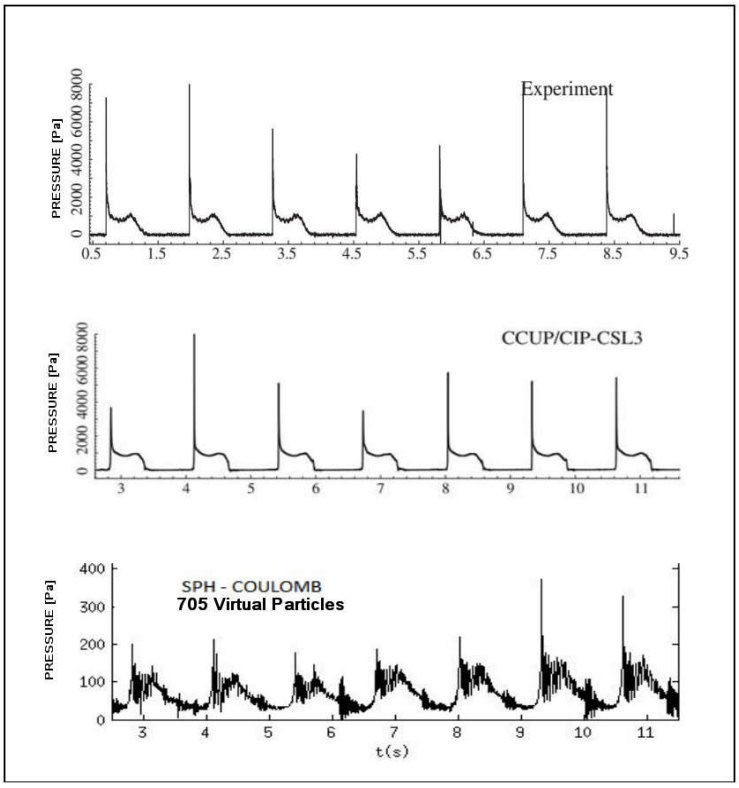


Figure 10. Parallel between physical experiment and numerical experiments for pressure data. Regarding the model applied to the SPH method, 705 virtual particles were used.

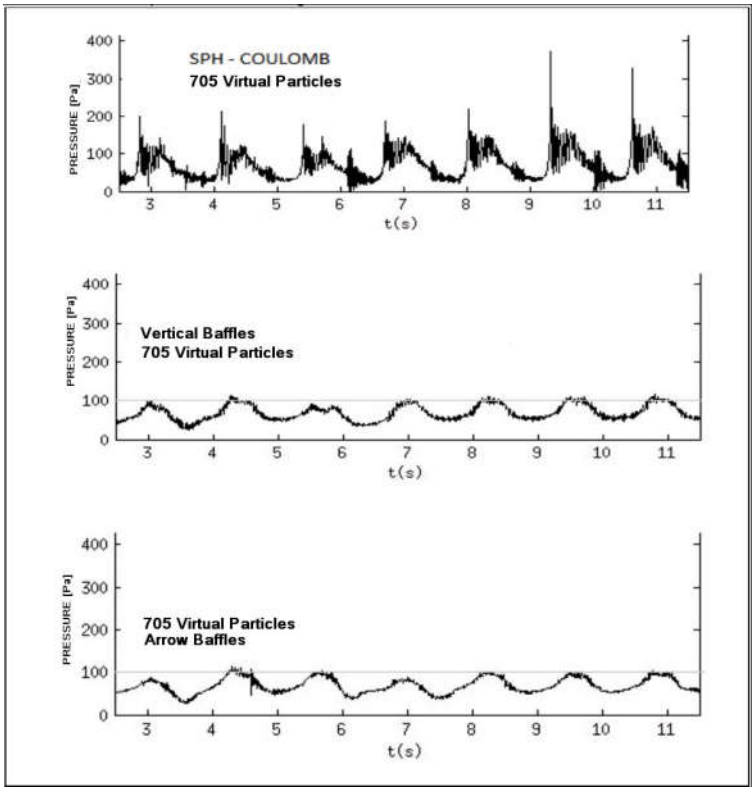


Figure 11- Pressure versus Time for three different scenarios

Figure 11 depicts Pressure versus Time for three different scenarios. The first top-down described above depicts the pressure behavior under the left tank wall at a point located at (x; y) = (0; 0.1). Following the figures the vertical is depicted and arrow shaped baffles in two separate tanks with their respective sloshing suppression mechanisms.

## 7 Conclusion

In this study, the number of particles used during the contour treatment was 705. Using this configuration, the suppression mechanisms, under the same flow conditions, were tested. It has been found that inadequate baffle height may lead to undesirable effects. Two heights were tested, in which the bulkhead with a height equal to 0.1 meters showed a good reduction in the hydrodynamic load on the walls.

In another scenario, the attenuation device took the form of an arrow. Both qualitatively and quantitatively, among all the baffles used, it proved to be more efficient as a suppression tool. The straight lines in (x; y) = (0; 100) and (12; 100) in Figure 9 were placed to visualize the variation between the highest point of pressure better. In this way, we conclude that for the level of the adopted filling, the baffle with the last configuration leads to a greater reduction of the effects produced by sloshing.

We agree with Tsukamoto (2010), when he states that deflectors are useless at high levels of filling. The bulkheads caused destructive interference in a dynamic behavior only at suitable heights

In all cases non-physical fluctuations of pressure appeared and edge effects were observed. Even with these numerical diffusions our model behaved effectively, reproducing with excellent approximations the qualitative and quantitative data, in this way, we can affirm that the underestimates did not cause damages to the results, with acceptable approximations when compared to their respective experiments. In addition, the arrow-shaped bafles presented a small improvement compared to the vertical deflectors for the same height, which is a strong indication that a more detailed study on the baffle morphology could generate a more significant reduction of the hydrodynamic loads on the walls.

## References

[1] POISSON S. D. Sur les petites oscillations de l'eau contenue dans un cylindre, *Ann. De Gergonne* XIX, 2225, (1828–9).

[2] RAYLEIGH J. W. S. (Lord). On the resistance of fluids, *Phil. Mag, 5 (2): 430 -441*. Reprinted in: *Scientific Papers* 1:287–296. 1876.

[3] LAMB, H. *HYDRODYNAMICS.* Cambridge University Press, pg 371, 1932.

[4] CHWANG, A. T. Effect of Hydrodynamic Interaction on the Motion of a Rotating Body. *J. of the Braz. Soc. of Mech*. Sci. & Eng. October-December 2004, Vol. XXVI, No. 4 / *349.* 2OO4.

[5] NASA, "Slosh Supression", Space Vehicle Design Criteria (estructures), NASA/SP-8031, 36 (1969). Available in:http://www.zerognews.com/special/sp8000/archive/ 00000024/01/sp8031.pdf. Accessed in: 02-20-2017.

[6] Graham. W. The Forces Produced by Fuel Oscillation in a Rectangular Tank. Front Cover. E.. Douglas Aircraft Company, Incorporated, 1951.

[7] O. R. Filho, "Estudo da influência do nível de alagamento sobre a estabilidade dinâmica de pesqueiros", Master's degree thesis (Naval and Oceanic engineering), Escola Politécnica, Universidade de São Paulo, doi:10.11606/D.3.2006.tde-19092006-165959, (2006). Available in: http://www.teses.usp.br/teses/disponiveis/3/3135/tde-19092006-165959/pt-br.php. Accessed in: 02-22-2017.

[8] IBRAHIM, R. A. *Liquid sloshing dynamics: theory and applications*. Cambridge University Press, 2005.

[9] CARNEIRO JUNIOR, D. P. *Comportamento de líquidos no espaço-sloshing e amortecedores de nutação viscosos*. Dissertação (Mestrado em Mecânica Espacial e Controle) - Instituto Nacional de Pesquisas Espaciais, São José dos Campos, 2009

[10] M. M. TSUKAMOTO, "Modelagem Analítica e Simulação Numérica de um Sistema de Supressão de Sloshing", Doctor's degree thesis (Naval and Oceanic engineering), Escola Politécnica, Universidade de São Paulo, doi: 10.11606/T.3.2011.tde-26082011-142211 (2010). Available in: http://www.teses.usp.br/teses/disponiveis/3/3135/tde-26082011-142211/pt-br.php. Accessed in: 02-22-2017.

[11] L. B. LUCY, "A numerical approach to the testing of the fission hypothesis", The Astronomical Journal 82 (12), 1013-1024 (1977).

[12] R. A. GINGOLD; J. J. MONAGHAN, "Smoothed particle hydrodynamics: theory and application to non-spherical stars", Monthly Notices of the Royal Astronomic Society 181 (3), 375-389 (1977).

[13] G. R. LIU; M. R. LIU, "Smooth Particle Hydrodynamics: A Meshfree Particle Method", *Word Scientific, 3rd printing* (2003).

[14] Z. R. KISHEV; C. HU; M. KASHIWAGI, "Numerical simulation of violent sloshing by a CIP-based method", Journal of Marine Science and Technology 11 (2), 111-122 (2006).

[15] H. GOTOH; A. KHAYYER A; H. IKARI H.; T. ARIKAWA; K. SHIMOSAKO, "On enhancement of Incompressible SPH method for simulation of violent sloshing flows", Applied Ocean Research 46, 104-115 (2014).

[16] D.A. Barbosa and F.P. Piccoli, Comparing the force due to the Lennard-Jones potential and the Coulomb force in the SPH Method, Journal of Ocean Engineering and Science, https://doi.org/10.1016/j.joes.2018.10.007.

[17] D.A. Barbosa and F.P. Piccoli,. REDUÇÃO DA CARGA HIDRODINÂMICA EM TANQUES POR ADIÇÃO DE DEFLETORES. In: XIII SIMMEC 2018 - Vitória - ES, 2018. Disponível em: <https://www.doity.com.br/anais/xiiisimmec2018/trabalho/65765>. Acesso em: 19/12/2018 às 23:25